RESEARCH PAPER

SYNTHESIS, CHARACTERIZATION AND MOLECULAR DOCKING ANALYSIS OF NOVEL THIAZOLE DERIVATIVES FOR ANTIBACTERIAL ACTIVITY

Jayshree S. Kokat[1*], Sanjay B. Bhawar[2]
[1]Department of pharmaceutical chemistry, Research scholar Bhagwant University, Ajmer
[2]Professor, Pravara Rural College of Pharmacy, Loni, Maharashtra, India

Corresponding Author
Jayshree Sudhakar Kokat
Department of Pharmaceutical Chemistry
Affiliation: Research scholar Bhagwant university, Ajmer
Email Id: jayshreekokat4@gmail.com
Mo No.: 8308210177

Abstract
Objectives: Type 2 diabetes mellitus remains a major global health burden with existing thiazolidinedione therapeutics limited by cardiovascular toxicity and hepatotoxicity. The present study aimed to design, synthesize, and characterize ten novel thiazolidinedione derivatives incorporating structurally diverse substituents and evaluate their antidiabetic potential through comprehensive in silico analysis targeting peroxisome proliferator-activated receptor gamma (PPARγ).
Methods: Ten novel derivatives (TZD01–TZD10) were synthesized via a two-step sequence comprising Knoevenagel condensation of 2,4-thiazolidinedione with substituted benzaldehydes followed by Michael addition with 4-(2-aminoethyl)morpholine. Structural characterization was performed by FT-IR, ^{1}H NMR, and ESI-MS. Drug-likeness, ADME, and toxicity profiles were predicted using ForceADME and Geintox-II platforms. Molecular docking against PPARγ (PDB: 2PRG) was performed using GeinDock Suite v2.5.7.
Results: All derivatives were obtained in yields of 66.3–75.3% and confirmed spectroscopically. Lipinski's Rule of Five assessment revealed one violation per compound, comparable to rosiglitazone, with molecular weights within 423.51–494.36 g/mol. All derivatives demonstrated high gastrointestinal absorption and absence of BBB penetration. Molecular docking identified TZD04, TZD07, and TZD09 as lead compounds with binding affinities of -8.85, -8.69, and -8.62 kcal/mol respectively against PPARγ, surpassing several reported antidiabetic scaffolds, with TZD04 engaging critical residues ARG288, SER342, CYS285, and HIS449.
Conclusion: The identified lead compounds TZD04, TZD07, and TZD09 demonstrate significant potential as safer PPARγ agonists with improved toxicity profiles compared to existing thiazolidinediones, warranting prioritization for in vitro and in vivo antidiabetic evaluation toward future clinical translation.
Keywords: Thiazolidinedione; PPARγ agonist; Type 2 diabetes; Molecular docking; In silico ADME; Drug design
How to cite this article: Kokat JS, Bhawar SB. Synthesis, Characterization and Molecular Docking Analysis of Novel Thiazole Derivatives for Antibacterial Activity. Int J Drug Deliv Technol. 2026;16(67s):1793-1813. DOI: 10.25258/ijddt.16.67s.162

Introduction

One of the most pressing challenges for global public health is antimicrobial resistance (AMR), which is the ability of pathogens to outsmart our conventional methods of antibiotic treatment, and more recently, bacterial pathogens are becoming more antimicrobial resistant. All across the world, multidrug-resistant Gram-positive and Gram-negative bacteria pose a challenge to routine clinical management and have been recognized as one of the top causes of morbidity and mortality by the World Health Organization on multiple occasions. The economic costs of these linked to long hospital stays, costly second-line treatments and premature death are billions of dollars a year in health systems [1]. The limitations of the existing antibacterial agents have increased, such as target mutation, efflux pump over-expression and the development of tolerance by the presence of biofilms, leading to the ineffectiveness of many first line drugs. This has been illustrated by recent epidemiological trends, showing an increase in resistant infections in community and hospital settings, with very few new chemical classes of antibacterials reaching clinical use in recent decades [2]. The ever increasing gap between emergence of resistance and drug discovery calls for urgent development of novel chemical scaffolds to overcome the existing resistance mechanisms [3, 4].

The five-member heterocycle thiazole, which contains both N and S atoms in its ring system has been of much interest in medicinal chemistry, because of the wide range of its biological activities [5]. The ring system has served as a structural

framework for many clinically important agents and is known to interact with a variety of biological targets via hydrogen bonding and hydrophobic interactions, provided by the heteroatoms. A number of studies have been reported on thiazole-containing compounds that show high activity towards bacterial, fungal, anti-inflammatory and anticancer activities [6, 7]. Thiazole derivatives in particular, with substituents other than those commonly used, have emerged as promising drugs against resistant bacterial strains; these inhibit the required enzymes and membrane integrity. The synthetic accessibility of the thiazole nucleus along with its excellent pharmacokinetic parameters and metabolic stability, has further strengthened its therapeutic value in various disease domains [8, 9].

A Structure Activity Relationship (SAR) analysis of thiazole derivatives suggests that the substitution at the second (2) and fourth (4) positions of the ring play a crucial role in determining the antibacterial activity [10]. Longer aromatic/heteroaromatic substitutions of the aryl substituent have generally made the molecule more active against the Gram-positive organisms and pi stacking interactions seem to be beneficial for target protein binding [11]. The advantage of thiazole based molecules is that these scaffolds can be diversified in several positions in systematic order and thereby, optimization of potency and selectivity can be achieved as compared to conventional antibacterial scaffolds. With the recent advances in synthetic methodologies, structually diverse and efficient libraries of thiazoles can be built, which can be used to rationally design new thiazoles via computational tools. All these advances have reinforced the scientific justification for exploring novel thiazole derivatives for the antibacterial targets which are decimating by resistance issues [12, 13].

The main aim of the present study is the synthesis of novel series of thiazole derivatives and systematic characterisation and molecular docking of their antibacterial potential. The most important aim is to develop a good SAR that can correlate between the substitution pattern and the antibacterial activity. In silico docking to the relevant target proteins in bacteria is also part of the secondary objectives to validate biological results. This synthetic and computational strategy is hoped to lead to the identification of potential lead compounds and provide insights into the mechanism by which these compounds are likely to exert their antibacterial activity.

Materials and Methods

Materials

4-(2-Bromoacetyl)benzene-1-carboxylic acid (analytical grade, MW 243.06 g/mol) and ethanethioamide (analytical grade, MW 75.13 g/mol) were procured from Sciquaint Chemicals, Pune, India. Thionyl chloride (analytical grade, purity ≥99%) and triethylamine (analytical grade, purity ≥99%) were obtained from Neeta Chemicals, Pune, India. All diversely substituted aniline precursors (TA1–TA25 series, analytical grade, purity ≥98%) were sourced from Research Lab Fine Chem Industries, Pune, India. Dry toluene (HPLC grade), dichloromethane (HPLC grade), and ethanol (analytical grade, purity ≥99.9%) used as reaction solvents were procured from Sciquaint Innovations (OPC) Pvt. Ltd., Pune, India. Potassium bromide (spectroscopic grade, purity ≥99%) for FT-IR pellet preparation and deuterated chloroform ($CDCl_3$, NMR grade, 99.8 atom % D) for NMR spectral analysis were also obtained from Sciquaint Chemicals, Pune, India. All other chemicals and reagents used in the study were of analytical grade and used without further purification unless otherwise specified.

Methods

Drug-Likeness and In-Silico ADME Prediction

The designed thiazole derivatives (TA1–TA25) were subjected to drug-likeness, and pharmacokinetic properties were calculated using the ForceADME (https://geinforce.com/force-adme/) web-based computational tool developed by Geinforce Technology Pvt. Ltd., Pune, India [14]. Two-dimensional SMILES strings of each compounds have been submitted to the platform where the Lipinski's rule of five parameters (MW, MLogP, HBDs, HBA, TPSA) and Veber's parameters (Countries rotatable bonds, TPSA) underwent calculations. Gastrointestinal absorption, blood-brain barrier penetration, P-glycoprotein substrate recognition, CYP inhibition profiles (CYP1A2, CYP2C19, CYP2C9, CYP2D6, CYP3A4), skin permeation coefficient (Log Kp) and bioavailability score were predicted simultaneously. Compliance of drug-likeness was further evaluated through Ghose, Egan and Muegge filters within the platform [15, 16].

Toxicity Prediction

Geintox-II (https://geinforce.com) is a web-based tool for toxicity prediction developed by Geinforce Technology Pvt. Ltd. Pune, India which has been used, in-silico toxicity assessment of all designed compounds was done. SMILES representations of each compound were entered into the tool, and for each compound, predictions of acute oral toxicity (expressed as LD50 (mg/kg)) and GHS toxicity class as well as endpoint-specific predictions including hepatotoxicity, carcinogenicity, mutagenicity, cytotoxicity, immunotoxicity, nephrotoxicity, cardiotoxicity, neurotoxicity, respiratory toxicity, skin sensitization, developmental toxicity and endocrine disruption, phospholipidosis, and ecotoxicity, and blood-brain barrier penetration were generated. The endpoints were given a probability score and high reliability rating based on literature-validated structural alert methods, which were reported as either active or inactive[17].

Ligand Preparation

To draw their two-dimensional (2D) structures, all the designed thiazole derivatives (TA1–TA25) and the reference standard Trimethoprim were plotted in the ChemDraw Professional (PerkinElmer Inc., USA) software. Before export, each structure was checked for the proper assignment of valencies, bonds orders and stereochemistry [18, 19]. The structures were saved as "MOL" files, which were then used as input files for the molecular docking studies.

Selection of Target Receptor

The crystal structure of Staphylococcus aureus dihydrofolate reductase (DHFR – PDB ID: 2W9H) was chosen as a target receptor for docking studies. DHFR catalyzes the NADPH-dependent reduction of dihydrofolate to tetrahydrofolate which is a necessary step in the folate biosynthesis of bacteria and a requisite for purine and thymidylate synthesis. Considerable efforts have been directed towards the inhibition of this enzyme for the broad-spectrum interruption of DNA replication and the proliferation of bacteria, and its inhibition has already been validated as an antibiotic target. The thiazole-benzamide scaffold was chosen for testing in this target because of its complementary shape to the DHFR active site, and the well-documented affinity of nitrogen-sulfur heterocycles to the folate-binding pocket of bacterial DHFR [20, 21].

Protein Preparation

The 3D crystal structure of Staphylococcus aureus DHFR (PDB ID: 2W9H) was downloaded from the RCSB Protein Data Bank (https://www.rcsb.org/). Processing of the downloaded structure was done using the visualizer software BIOVA Discovery Studio Visualizer v4.5. The water molecules and heteroatoms have been stripped from the structure to give the apo-protein. The fine structure of the protein was stored in PDB format and utilized as the receptor for following molecular docking calculations [22].

Molecular Docking

The docking of all synthesized thiazole derivatives (TA1–TA25) was achieved using a desktop docking software GeinDock Suite v2.5.6 (https://geindock.geinforce.com/). MOL files of the prepared ligands and PDB file of the receptor were uploaded to the application interface [23]. The docking box was set on bound ligand conformation of was selected and docking grid center was set at x = 8.96, y = −5.92, z = 16.43 and dimensions of x = 20, y = 21.8, z = 21.8Å. Before docking of test compounds, validation of the protocol was carried out by using the co-crystallized reference ligand Trimethoprim which was re-docked into the specified grid, with the grid accepted based on the RMSD of less than 2.0 Å between the redocked and co-crystallized poses. Docking scores were reported as kcal/mol and possible interactions such as hydrogen bonds, hydrophobic bonds, electrostatic interactions, halogen bonds, and Van der Waals interactions were identified and displayed using the BIOVA Discovery Studio Visualizer v4.5.[24]

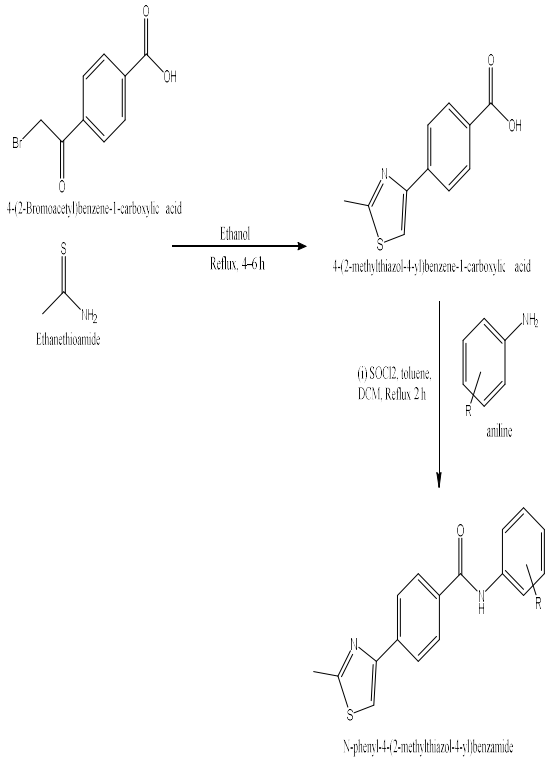

Figure 1: Proposed scheme I for synthesis of Thiazole derivatives

Table 1: Designed novel thiazole derivatives (TA1–TA25) with corresponding aniline substituents and IUPAC names of final products synthesized via Scheme I.

Label	R - Substitution	IUPAC Name of Final Product
TA1	4-Fluoro-3-(trifluoromethyl)aniline	N-[4-fluoro-3-(trifluoromethyl)phenyl]-4-(2-methylthiazol-4-yl)benzamide
TA2	3,5-Dichloro-4-methylaniline	N-(3,5-dichloro-4-methylphenyl)-4-(2-methylthiazol-4-yl)benzamide
TA3	4-Bromo-3-chloro-5-fluoroaniline	N-(4-bromo-3-chloro-5-fluorophenyl)-4-(2-methylthiazol-4-yl)benzamide
TA4	2-Chloro-5-fluoro-4-(trifluoromethoxy) aniline	N-[2-chloro-5-fluoro-4-(trifluoromethoxy)phenyl]-4-(2-methylthiazol-4-yl)benzamide

TA 5	2,6-Difluoro-4-(methylsulfonyl)aniline	N-[2,6-difluoro-4-(methylsulfonyl)phenyl]-4-(2-methylthiazol-4-yl)benzamide
TA 6	3-(Difluoromethoxy)-4-fluoroaniline	N-[3-(difluoromethoxy)-4-fluorophenyl]-4-(2-methylthiazol-4-yl)benzamide
TA 7	4-(Cyclopropylmethoxy)-3-(trifluoromethyl)aniline	N-[4-(cyclopropylmethoxy)-3-(trifluoromethyl)phenyl]-4-(2-methylthiazol-4-yl)benzamide
TA 8	3-Methoxy-4-(trifluoromethyl)aniline	N-[3-methoxy-4-(trifluoromethyl)phenyl]-4-(2-methylthiazol-4-yl)benzamide
TA 9	2-Fluoro-4-(2,2,2-trifluoroethoxy)aniline	N-[2-fluoro-4-(2,2,2-trifluoroethoxy)phenyl]-4-(2-methylthiazol-4-yl)benzamide
TA 10	3-Chloro-4-(cyclobutyloxy)aniline	N-[3-chloro-4-(cyclobutyloxy)phenyl]-4-(2-methylthiazol-4-yl)benzamide
TA 11	2-Fluoro-4-(1-methyl-1H-pyrazol-4-yl)aniline	N-[2-fluoro-4-(1-methyl-1H-pyrazol-4-yl)phenyl]-4-(2-methylthiazol-4-yl)benzamide
TA 12	3-Fluoro-4-(1,3-oxazol-5-yl)aniline	N-[3-fluoro-4-(1,3-oxazol-5-yl)phenyl]-4-(2-methylthiazol-4-yl)benzamide
TA 13	4-(5-Methyl-1,2,4-oxadiazol-3-yl)aniline	N-[4-(5-methyl-1,2,4-oxadiazol-3-yl)phenyl]-4-(2-methylthiazol-4-yl)benzamide
TA 14	4-Fluoro-3-(1-methyl-1H-imidazol-4-yl)aniline	N-[4-fluoro-3-(1-methyl-1H-imidazol-4-yl)phenyl]-4-(2-methylthiazol-4-yl)benzamide
TA 15	2-Chloro-4-(3-methylisoxazol-5-yl)aniline	N-[2-chloro-4-(3-methylisoxazol-5-yl)phenyl]-4-(2-methylthiazol-4-yl)benzamide
TA 16	3-Fluoro-4-(ethylsulfonyl)aniline	N-[3-fluoro-4-(ethylsulfonyl)phenyl]-4-(2-methylthiazol-4-yl)benzamide
TA 17	3-Chloro-4-[(dimethylamino)sulfonyl]aniline	N-{3-chloro-4-[(dimethylamino)sulfonyl]phenyl}-4-(2-methylthiazol-4-yl)benzamide
TA 18	3,5-Dimethyl-4-(methylsulfonyl)aniline	N-[3,5-dimethyl-4-(methylsulfonyl)phenyl]-4-(2-methylthiazol-4-yl)benzamide
TA 19	4-(Isopropylsulfonyl)-3-(trifluoromethyl)aniline	N-[4-(isopropylsulfonyl)-3-(trifluoromethyl)phenyl]-4-(2-methylthiazol-4-yl)benzamide
TA 20	4-Chloro-2-fluoro-5-(methylsulfonyl)aniline	N-[4-chloro-2-fluoro-5-(methylsulfonyl)phenyl]-4-(2-methylthiazol-4-yl)benzamide
TA 21	3-Cyclopropyl-4-(trifluoromethyl)aniline	N-[3-cyclopropyl-4-(trifluoromethyl)phenyl]-4-(2-methylthiazol-4-yl)benzamide
TA 22	4-(Difluoromethoxy)-2-(trifluoromethyl)aniline	N-[4-(difluoromethoxy)-2-(trifluoromethyl)phenyl]-4-(2-methylthiazol-4-yl)benzamide
TA 23	3-Fluoro-4-(methylthio)-5-(trifluoromethyl)aniline	N-[3-fluoro-4-(methylthio)-5-(trifluoromethyl)phenyl]-4-(2-methylthiazol-4-yl)benzamide
TA 24	4-Chloro-3-(2-fluoroethyl)aniline	N-[4-chloro-3-(2-fluoroethyl)phenyl]-4-(2-methylthiazol-4-yl)benzamide
TA 25	3-Fluoro-4-[(dimethylamino)carbonyl]aniline	N-{3-fluoro-4-[(dimethylamino)carbonyl]phenyl}-4-(2-methylthiazol-4-yl)benzamide

Synthesis and Characterization of Thiazole derivatives

Synthesis of N-[4-fluoro-3-(trifluoromethyl)phenyl]-4-(2-methylthiazol-4-yl)benzamide (TA1)

In a 100 mL round bottom flask, 4-(2-methylthiazol-4-yl)benzoic acid (0.219 g, 1.0 mmol) was dissolved in dry toluene (15 mL) and thionyl chloride (0.145 mL, 2.0 mmol) was added dropwise. The mixture was refluxed at 80 °C for 2 h under nitrogen atmosphere and the solvent along with excess thionyl chloride was removed under reduced pressure. The acid chloride residue was dissolved in dry DCM (10 mL). In a separate flask, 4-fluoro-3-(trifluoromethyl)aniline (0.179 g, 1.0 mmol) was dissolved in dry DCM (10 mL) containing triethylamine (0.28 mL, 2.0 mmol) and cooled to 0 °C. The acid chloride solution was added dropwise and the reaction was stirred at room temperature for 12 h.

Off-white solid; Yield: 0.318 g (76%); m.p. 183–186 °C. FT-IR (KBr) (cm^{-1}): 3316.48 (N-H amide), 3084.62 (Ar-H), 2926.73 (C-H aliphatic), 1654.27 (C=O amide), 1596.43 (C=C aromatic), 1542.87 (C=N thiazole), 1306.54 (C-N), 1282.36 (C-F), 1224.18 (C-F aromatic), 1064.72 ($C-F_3$), 838.47 (C-H out-of-plane). ^1H NMR (500 MHz, $CDCl_3$) δ: 9.86 (s, 1H, NH), 8.13 (d, J = 8.6 Hz, 2H, Ar-H), 8.02 (dd, J = 6.7, 2.6 Hz, 1H, Ar-H), 7.91 (d, J = 8.6 Hz, 2H, Ar-H), 7.78 (ddd, J = 8.7, 4.4, 2.6 Hz, 1H, Ar-H), 7.42 (s, 1H, thiazole-H), 7.26 (t, J = 9.6 Hz, 1H, Ar-H), 2.63 (s, 3H, thiazole-CH_3). ^{13}C NMR (125 MHz, $CDCl_3$) δ: 176.34, 165.46, 154.82 (d, J = 252.4 Hz, C-F), 143.74, 140.58, 138.64, 135.32, 134.81, 132.62, 129.87, 128.56, 127.43, 124.18 (q, J = 32.6 Hz, C-CF_3), 122.52, 122.27 (q, J = 271.8 Hz, CF_3), 120.34, 116.82 (d, J = 21.4 Hz), 19.22. ESI-MS (m/z): 381.37 $[M+H]^+$ [25].

Synthesis of N-[2-fluoro-4-(1-methyl-1H-pyrazol-4-yl)phenyl]-4-(2-methylthiazol-4-yl)benzamide (TA11)

In a 100 mL round bottom flask, 4-(2-methylthiazol-4-yl)benzoic acid (0.219 g, 1.0 mmol) was dissolved in dry toluene (15 mL) and thionyl chloride (0.145 mL, 2.0 mmol) was added. The mixture was refluxed at 80 °C for 2 h. The solvent was evaporated under reduced pressure and the acid chloride residue was dissolved in dry DCM (10 mL). Separately, 2-fluoro-4-(1-methyl-1H-pyrazol-4-yl)aniline (0.191 g, 1.0 mmol) was dissolved in dry DCM (10 mL) with triethylamine (0.28 mL, 2.0 mmol). The acid chloride solution was added dropwise at 0 °C and stirring was continued at room temperature for 12 h.

Off-white solid; Yield: 0.362 g (82%); m.p. 198–201 °C. FT-IR (KBr) (cm^{-1}): 3312.17 (N-H amide), 3094.83 (Ar-H), 2931.46 (C-H aliphatic), 1661.58 (C=O amide), 1604.23 (C=C aromatic), 1542.76 (C=N thiazole), 1498.34 (C=N pyrazole), 1318.47 (C-N), 1224.63 (C-F), 821.45 (C-H out-of-plane). ^1H NMR (500 MHz, $CDCl_3$) δ: 9.76 (s, 1H, NH), 8.09 (d, J = 8.5 Hz, 2H, Ar-H), 7.94 (s, 1H, pyrazole-H), 7.87 (d, J = 8.6 Hz, 2H, Ar-H), 7.74 (s, 1H, pyrazole-H), 7.52 (t, J = 8.2 Hz, 1H, Ar-H), 7.38 (s, 1H, thiazole-H), 7.21 (dd, J = 8.3, 1.6 Hz, 1H, Ar-H), 7.14 (dd, J = 12.4, 1.6 Hz, 1H, Ar-H), 3.92 (s, 3H, N-CH_3), 2.59 (s, 3H, thiazole-CH_3). ^{13}C NMR (125 MHz, $CDCl_3$) δ: 176.18, 165.43, 157.34 (d, J = 248.2 Hz, C-F), 143.52, 140.87, 138.94, 135.16, 134.61, 132.47, 130.82, 129.58, 128.73, 127.44, 122.63, 119.38, 116.74 (d, J = 3.1 Hz), 114.28 (d, J = 14.6 Hz), 39.14, 19.12. ESI-MS (m/z): 393.46 $[M+H]^+$ [26].

Synthesis of N-[3-fluoro-4-(1,3-oxazol-5-yl)phenyl]-4-(2-methylthiazol-4-yl)benzamide (TA12)

In a 100 mL round bottom flask, 4-(2-methylthiazol-4-yl)benzoic acid (0.219 g, 1.0 mmol) was dissolved in dry toluene (15 mL) and thionyl chloride (0.145 mL, 2.0 mmol) was added. The mixture was heated under reflux at 80 °C for 2 h and the volatiles were removed under reduced pressure. The resulting acid chloride was dissolved in dry DCM (10 mL). 3-Fluoro-4-(1,3-oxazol-5-yl)aniline (0.178 g, 1.0 mmol) dissolved in dry DCM (10 mL) containing triethylamine (0.28 mL, 2.0 mmol) was cooled to 0 °C and the acid chloride solution was added dropwise. The reaction mixture was allowed to warm to room temperature and stirred for 12 h.

Light yellow solid; Yield: 0.334 g (76%); m.p. 207–210 °C. FT-IR (KBr) (cm^{-1}): 3304.58 (N-H amide), 3078.24 (Ar-H), 2918.67 (C-H aliphatic), 1656.84 (C=O amide), 1598.36 (C=C aromatic), 1544.13 (C=N thiazole), 1492.57 (C=N oxazole), 1316.82 (C-N), 1218.74 (C-F), 1136.29 (C-O oxazole), 836.54 (C-H out-of-plane). ^1H NMR (500 MHz, $CDCl_3$) δ: 9.79 (s, 1H, NH), 8.11 (d, J = 8.6 Hz, 2H, Ar-H), 7.97 (s, 1H, oxazole-H-2), 7.89 (d, J = 8.6 Hz, 2H, Ar-H), 7.68 (t, J = 8.3 Hz, 1H, Ar-H), 7.56 (s, 1H, oxazole-H-4), 7.42 (s, 1H, thiazole-H), 7.38 (dd, J = 8.4, 2.1 Hz, 1H, Ar-H), 7.24 (dd, J = 11.8, 2.1 Hz, 1H, Ar-H), 2.62 (s, 3H, thiazole-CH_3). ^{13}C NMR (125 MHz, $CDCl_3$) δ: 176.24, 165.67, 156.82 (d, J = 246.7 Hz, C-F), 151.43, 143.68, 140.23, 138.47, 135.28, 134.73, 132.61, 129.84, 128.52, 127.36, 122.47, 120.16, 117.63, 114.52 (d, J = 3.4 Hz), 112.38 (d, J = 15.1 Hz), 19.18. ESI-MS (m/z): 380.41 $[M+H]^+$ [27].

Synthesis of N-[4-(5-methyl-1,2,4-oxadiazol-3-yl)phenyl]-4-(2-methylthiazol-4-yl)benzamide (TA13)

In a 100 mL round bottom flask, 4-(2-methylthiazol-4-yl)benzoic acid (0.219 g, 1.0 mmol) was dissolved in dry toluene (15 mL), followed by addition of thionyl chloride (0.145 mL, 2.0 mmol). The reaction mixture was refluxed at 80 °C for 2 h under anhydrous conditions to yield the corresponding acid chloride intermediate. The solvent and excess thionyl chloride were removed under reduced pressure and the residue was redissolved in dry DCM (10 mL). In a separate flask, 4-(5-methyl-1,2,4-oxadiazol-3-yl)aniline (0.175 g, 1.0 mmol) was dissolved in dry DCM (10 mL) and triethylamine (0.28 mL, 2.0 mmol) was added. The acid chloride solution was added dropwise to the

aniline solution at 0 °C and the mixture was stirred at room temperature for 12 h.

Pale yellow solid; Yield: 0.348 g (79%); m.p. 214–216 °C. FT-IR (KBr) (cm^{-1}): 3298.42 (N-H amide), 3087.61 (Ar-H), 2924.35 (C-H aliphatic), 1658.23 (C=O amide), 1601.47 (C=C aromatic), 1548.92 (C=N thiazole), 1496.18 (C=N oxadiazole), 1312.54 (C-N), 1178.36 (C-O oxadiazole), 854.72 (C-H out-of-plane). ^{1}H NMR (500 MHz, $CDCl_3$) δ: 9.84 (s, 1H, NH), 8.12 (d, J = 8.6 Hz, 2H, Ar-H), 7.98 (d, J = 8.7 Hz, 2H, Ar-H), 7.86 (d, J = 8.7 Hz, 2H, Ar-H), 7.72 (d, J = 8.6 Hz, 2H, Ar-H), 7.41 (s, 1H, thiazole-H), 2.68 (s, 3H, oxadiazole-CH_3), 2.61 (s, 3H, thiazole-CH_3). ^{13}C NMR (125 MHz, $CDCl_3$) δ: 176.42, 167.83, 165.12, 163.47, 154.28, 143.67, 139.14, 134.82, 132.56, 129.73, 129.41, 128.94, 127.63, 122.18, 119.47, 116.82, 19.24, 12.37. ESI-MS (m/z): 377.42 $[M+H]^+$.[28]

Synthesis of N-[4-fluoro-3-(1-methyl-1H-imidazol-4-yl)phenyl]-4-(2-methylthiazol-4-yl)benzamide (TA14)

In a 100 mL round bottom flask, 4-(2-methylthiazol-4-yl)benzoic acid (0.219 g, 1.0 mmol) was dissolved in dry toluene (15 mL) and thionyl chloride (0.145 mL, 2.0 mmol) was added. The mixture was heated at 80 °C for 2 h under reflux conditions and the solvent was evaporated under reduced pressure. The acid chloride residue was dissolved in dry DCM (10 mL). 4-Fluoro-3-(1-methyl-1H-imidazol-4-yl)aniline (0.191 g, 1.0 mmol) dissolved in dry DCM (10 mL) with triethylamine (0.28 mL, 2.0 mmol) was cooled to 0 °C, the acid chloride was added dropwise and the mixture was stirred at room temperature for 12 h.

Light brown solid; Yield: 0.344 g (79%); m.p. 204–207 °C. FT-IR (KBr) (cm^{-1}): 3318.56 (N-H amide), 3096.43 (Ar-H), 2936.74 (C-H aliphatic), 1658.84 (C=O amide), 1602.37 (C=C aromatic), 1544.62 (C=N thiazole), 1496.28 (C=N imidazole), 1314.83 (C-N), 1226.47 (C-F), 824.36 (C-H out-of-plane). ^{1}H NMR (500 MHz, $CDCl_3$) δ: 9.78 (s, 1H, NH), 8.10 (d, J = 8.5 Hz, 2H, Ar-H), 7.92 (d, J = 2.3 Hz, 1H, imidazole-H), 7.88 (d, J = 8.5 Hz, 2H, Ar-H), 7.74 (s, 1H, imidazole-H), 7.56 (dd, J = 7.2, 2.3 Hz, 1H, Ar-H), 7.42 (s, 1H, thiazole-H), 7.38 (ddd, J = 8.6, 4.3, 2.3 Hz, 1H, Ar-H), 7.18 (t, J = 9.4 Hz, 1H, Ar-H), 3.74 (s, 3H, N-CH_3), 2.61 (s, 3H, thiazole-CH_3). ^{13}C NMR (125 MHz, $CDCl_3$) δ: 176.22, 165.48, 156.74 (d, J = 247.8 Hz, C-F), 143.58, 140.38, 138.62, 136.84, 135.24, 134.67, 132.52, 129.76, 128.54, 127.42, 122.44, 120.38, 118.62, 116.74 (d, J = 3.2 Hz), 114.36 (d, J = 14.8 Hz), 33.84, 19.16. ESI-MS (m/z): 393.46 $[M+H]^+$ [29].

Synthesis of N-[2-chloro-4-(3-methylisoxazol-5-yl)phenyl]-4-(2-methylthiazol-4-yl)benzamide (TA15)

In a 100 mL round bottom flask, 4-(2-methylthiazol-4-yl)benzoic acid (0.219 g, 1.0 mmol) was dissolved in dry toluene (15 mL) and thionyl chloride (0.145 mL, 2.0 mmol) was added. The mixture was refluxed at 80 °C for 2 h under nitrogen atmosphere and the solvent was removed under reduced pressure. The acid chloride residue was dissolved in dry DCM (10 mL). 2-Chloro-4-(3-methylisoxazol-5-yl)aniline (0.208 g, 1.0 mmol) dissolved in dry DCM (10 mL) with triethylamine (0.28 mL, 2.0 mmol) was cooled to 0 °C and the acid chloride was added dropwise. The mixture was stirred at room temperature for 12 h.

Pale yellow solid; Yield: 0.356 g (78%); m.p. 228–231 °C. FT-IR (KBr) (cm^{-1}): 3308.64 (N-H amide), 3091.37 (Ar-H), 2934.82 (C-H aliphatic), 1659.43 (C=O amide), 1602.18 (C=C aromatic), 1546.84 (C=N thiazole), 1494.36 (C=N isoxazole), 1312.57 (C-N), 1136.43 (C-O isoxazole), 752.68 (C-Cl). ^{1}H NMR (500 MHz, $CDCl_3$) δ: 9.88 (s, 1H, NH), 8.16 (d, J = 8.6 Hz, 2H, Ar-H), 8.04 (d, J = 2.2 Hz, 1H, Ar-H), 7.91 (d, J = 8.6 Hz, 2H, Ar-H), 7.72 (dd, J = 8.3, 2.2 Hz, 1H, Ar-H), 7.48 (d, J = 8.3 Hz, 1H, Ar-H), 7.44 (s, 1H, thiazole-H), 6.42 (s, 1H, isoxazole-H), 2.64 (s, 3H, thiazole-CH_3), 2.28 (s, 3H, isoxazole-CH_3). ^{13}C NMR (125 MHz, $CDCl_3$) δ: 176.36, 168.47, 165.54, 162.83, 143.72, 140.34, 138.82, 135.43, 134.68, 132.54, 131.27, 129.74, 128.63, 127.48, 122.36, 120.54, 116.73, 100.42, 19.21, 11.64. ESI-MS (m/z): 410.88 $[M+H]^+$ [30].

Synthesis of N-[4-(isopropylsulfonyl)-3-(trifluoromethyl)phenyl]-4-(2-methylthiazol-4-yl)benzamide (TA19)

In a 100 mL round bottom flask, 4-(2-methylthiazol-4-yl)benzoic acid (0.219 g, 1.0 mmol) was taken up in dry toluene (15 mL) and thionyl chloride (0.145 mL, 2.0 mmol) was added. The mixture was refluxed at 80 °C for 2 h. The volatiles were removed under reduced pressure and the acid chloride residue was dissolved in dry DCM (10 mL). In a separate flask, 4-(isopropylsulfonyl)-3-(trifluoromethyl)aniline (0.267 g, 1.0 mmol) was dissolved in dry DCM (10 mL) with triethylamine (0.28 mL, 2.0 mmol) at 0 °C. The acid chloride solution was added dropwise and the reaction mixture was stirred at room temperature for 12 h.

White solid; Yield: 0.387 g (74%); m.p. 221–224 °C. FT-IR (KBr) (cm^{-1}): 3286.43 (N-H amide), 3082.17 (Ar-H), 2978.54 (C-H aliphatic), 1663.72 (C=O amide), 1596.84 (C=C aromatic), 1546.29 (C=N thiazole), 1314.63 (C-N), 1298.47 (C-F), 1174.82 (S=O), 1132.56 (C-SO_2), 1072.34 (C-F_3). ^{1}H NMR (500 MHz, $CDCl_3$) δ: 9.94 (s, 1H, NH), 8.28 (d, J = 2.1 Hz, 1H, Ar-H), 8.14 (d, J = 8.5 Hz, 2H, Ar-H), 8.03 (dd, J = 8.6, 2.1 Hz, 1H, Ar-H), 7.92 (d, J = 8.6 Hz, 1H, Ar-H), 7.88 (d, J = 8.5 Hz, 2H, Ar-H), 7.43 (s, 1H, thiazole-H), 3.24 (hept, J = 6.8 Hz, 1H, $CH(CH_3)_2$), 2.63 (s, 3H, thiazole-CH_3), 1.31 (d, J = 6.8 Hz, 6H, $CH(CH_3)_2$). ^{13}C NMR (125 MHz, $CDCl_3$) δ: 176.53, 165.28, 143.84, 140.62, 138.73, 136.24, 134.92, 132.78, 131.47, 129.96, 128.84, 127.52, 126.43 (q, J = 32.4 Hz, C-CF_3), 122.84, 122.56 (q, J = 273.6 Hz, CF_3), 120.17, 55.43, 19.26, 14.87. ESI-MS (m/z): 469.52 $[M+H]^+$.[31]

Synthesis of N-[3-cyclopropyl-4-(trifluoromethyl)phenyl]-4-(2-methylthiazol-4-yl)benzamide (TA21)

In a 100 mL round bottom flask, 4-(2-methylthiazol-4-yl)benzoic acid (0.219 g, 1.0 mmol) was dissolved in dry toluene (15 mL) and thionyl chloride (0.145 mL, 2.0 mmol) was added. The mixture was refluxed at 80 °C for 2 h and the solvent was evaporated under reduced pressure. The resulting acid chloride was dissolved in dry DCM (10 mL). 3-Cyclopropyl-4-(trifluoromethyl)aniline (0.201 g, 1.0 mmol) was dissolved in dry DCM (10 mL) with triethylamine (0.28 mL, 2.0 mmol) at 0 °C and the acid chloride solution was added dropwise with stirring. The mixture was allowed to reach room temperature and stirred for 12 h.

White solid; Yield: 0.341 g (77%); m.p. 196–199 °C. FT-IR (KBr) (cm^{-1}): 3294.27 (N-H amide), 3072.48 (Ar-H), 2962.83 (C-H aliphatic), 1657.36 (C=O amide), 1598.74 (C=C aromatic), 1544.18 (C=N thiazole), 1308.62 (C-N), 1286.47 (C-F), 1068.93 (C-F_3), 842.36 (C-H out-of-plane). ^{1}H NMR (500 MHz, $CDCl_3$) δ: 9.82 (s, 1H, NH), 8.12 (d, J = 8.5 Hz, 2H, Ar-H), 7.89 (d, J = 8.5 Hz, 2H, Ar-H), 7.74 (d, J = 8.4 Hz, 1H, Ar-H), 7.62 (d, J = 2.1 Hz, 1H, Ar-H), 7.41 (s, 1H, thiazole-H), 7.34 (dd, J = 8.4, 2.1 Hz, 1H, Ar-H), 2.62 (s, 3H, thiazole-CH_3), 1.94 (tt, J = 8.4, 5.2 Hz, 1H, cyclopropyl-CH), 1.06 (m, 2H, cyclopropyl-CH_2), 0.82 (m, 2H, cyclopropyl-CH_2). ^{13}C NMR (125 MHz, $CDCl_3$) δ: 176.28, 165.38, 143.61, 140.47, 138.56, 137.84, 134.74, 132.43, 129.68, 128.47, 127.34, 124.62 (q, J = 31.8 Hz, C-CF_3), 122.38, 122.14 (q, J = 272.4 Hz, CF_3), 120.26, 117.43, 19.14, 9.82, 8.64. ESI-MS (m/z): 403.43 $[M+H]^+$[32].

Synthesis of N-[4-(difluoromethoxy)-2-(trifluoromethyl)phenyl]-4-(2-methylthiazol-4-yl)benzamide (TA22)

In a 100 mL round bottom flask, 4-(2-methylthiazol-4-yl)benzoic acid (0.219 g, 1.0 mmol) was dissolved in dry toluene (15 mL) and thionyl chloride (0.145 mL, 2.0 mmol) was added. The mixture was refluxed at 80 °C for 2 h and the solvent was removed under reduced pressure. The acid chloride residue was dissolved in dry DCM (10 mL). 4-(Difluoromethoxy)-2-(trifluoromethyl)aniline (0.227 g, 1.0 mmol) was dissolved in dry DCM (10 mL) containing triethylamine (0.28 mL, 2.0 mmol) at 0 °C and the acid chloride solution was added dropwise. The reaction mixture was stirred at room temperature for 12 h.

Pale yellow solid; Yield: 0.372 g (78%); m.p. 176–179 °C. FT-IR (KBr) (cm^{-1}): 3302.83 (N-H amide), 3086.47 (Ar-H), 2944.62 (C-H aliphatic), 1661.48 (C=O amide), 1600.27 (C=C aromatic), 1548.63 (C=N thiazole), 1318.74 (C-N), 1284.52 (C-F), 1218.36 (O-CF_2H), 1076.84 (C-F_3), 836.29 (C-H out-of-plane). ^{1}H NMR (500 MHz, $CDCl_3$) δ: 9.91 (s, 1H, NH), 8.15 (d, J = 8.5 Hz, 2H, Ar-H), 7.93 (d, J = 8.5 Hz, 2H, Ar-H), 7.68 (d, J = 8.7 Hz, 1H, Ar-H), 7.54 (d, J = 2.6 Hz, 1H, Ar-H), 7.43 (s, 1H, thiazole-H), 7.38 (dd, J = 8.7, 2.6 Hz, 1H, Ar-H), 6.58 (t, J = 74.2 Hz, 1H, OCF_2H), 2.63 (s, 3H, thiazole-CH_3). ^{13}C NMR (125 MHz, $CDCl_3$) δ: 176.41, 165.52, 148.36, 143.78, 140.64, 138.72, 134.86, 132.67, 129.92, 128.62, 127.48, 124.34 (q, J = 31.6 Hz, C-CF_3), 122.58, 122.34 (q, J = 272.7 Hz, CF_3), 121.46, 118.73, 116.34, 114.28 (t, J = 261.4 Hz, OCF_2H), 19.27. ESI-MS (m/z): 429.37 $[M+H]^+$[33].

Results and Discussion

Results

Calculations of Lipinski's rule of Five and Druglikeness

The Lipinski's Rule of five (RO5) and Veber's Rule parameters of all thiazole derivatives (TA1 – TA25) and reference standard "Trimethoprim" are listed in Table 2. All compounds had molecular weight ranges from 374.87 g/mol (TA24) to 468.52 g/mol (TA19) which falls within the accepted molecular weight range of 500 g/mol. The MLogP value varied between 1.45 (TA11) and 3.31 (TA4, TA22) which is below the threshold of 5 showing favourable Lipophilicity. For each compound, one HBD and three to six HBAs were found with the same Lipinski violation occurring throughout the series. TPSA varied between 41.99 Å2 to 80.91 Å2 with the number of rotatable bonds ranging from 4 to 8, which were in line with Veber's rule for predicting oral bioavailability of ≤140 Å2 and ≤10 rotatable bonds, respectively. Compared to the series of designed compounds, trimethoprim was also characterized by higher TPSA (105.51 Å²) and rotatable bonds (10).

Table 2: Lipinski's Rule of Five and Veber's Rule Parameters for All Compounds

Comp. Name	MLogP	Mol. Wt. (g/mol)	HBA	HBD	Violations	Total Polar Surface Area (Å²)	No. of Rotatable Bonds
TA1	2.96	380.37	3	1	1	41.99	4
TA2	2.47	377.3	3	1	1	41.99	5
TA3	2.82	425.71	3	1	1	41.99	4
TA4	3.31	430.81	4	1	1	51.22	5

TA5	2.56	408.45	5	1	1	76.13	6
TA6	2.69	378.37	4	1	1	51.22	6
TA7	3.04	432.47	4	1	1	51.22	7
TA8	2.73	392.4	4	1	1	51.22	6
TA9	3.02	410.39	4	1	1	51.22	6
TA10	2.46	398.91	4	1	1	51.22	6
TA11	1.45	392.46	5	1	1	59.81	6
TA12	2.17	379.42	5	1	1	68.02	5
TA13	1.55	376.44	6	1	1	80.91	6
TA14	1.87	392.46	5	1	1	59.81	6
TA15	2.26	409.9	5	1	1	68.02	6
TA16	2.32	404.49	5	1	1	76.13	7
TA17	2.02	435.96	5	1	1	79.37	8
TA18	2.07	400.52	5	1	1	76.13	8
TA19	2.99	468.52	5	1	1	76.13	8
TA20	2.6	424.91	5	1	1	76.13	6
TA21	2.98	402.44	3	1	1	41.99	5
TA22	3.31	428.38	4	1	1	51.22	6
TA23	3.06	426.46	4	1	1	41.99	6
TA24	2.48	374.87	3	1	1	41.99	6
TA25	1.91	383.45	4	1	1	62.3	7
Trimethoprim	-0.41	290.32	7	2	1	105.51	10

Mol. Wt.: Molecular weight; HBA: Hydrogen bond acceptors; HBD: Hydrogen bond donors; TPSA: Total polar surface area.

***In-silico* ADME properties**

The in-silico ADME and pharmacokinetic profiles of all synthesized thiazole derivatives (TA1–TA25) along with Trimethoprim are summarized in Table 3. There was also high gastrointestinal absorption for all 25 compounds with favorable oral bioavailability throughout the series. None of the compounds fell into the class of P-glycoprotein substrates and might be less prone to efflux resistance. Ten compounds (TA1, TA3, TA5, TA6, TA8, TA9, TA11, TA14, TA24, TA25) were predicted to be BBB-penetrant and the remaining fifteen were not predicted to penetrate the BBB — acceptable for peripherally acting antibacterial agents. For each series, all compounds were found to block both CYP1A2 and CYP2C9 isoforms uniformly, with no CYP2C19 type inhibition found in any of the series. Interestingly, only the TA17 had inhibitory activity on CYP2D6, which may be considered for the next metabolic safety screen. CYP3A4 was inhibited by all of the compounds. Moderate transdermal permeability was reflected in skin permeation values (Log Kp) with a range of −0.70 (TA21) to −2.33 (TA17). However, most of the compounds had a bioavailability of 0.85 with 0.55 for TA17, TA18 and TA19, which are closer to the value of Trimethoprim indicating that the predicted oral exposure for these three derivatives is lower. As expected, no compounds passed through Ghose, Egan, or Muegge drug-likeness "filters", which are based on the idea that such features as sulfonyls and halogens are beyond the limits.

Table 3: Pharmacokinetics and Drug-likeness Properties of All Compounds

Compound Name	GI abs.	BBB pen.	P-gp sub.	CYP1A2 inhibi	CYP2C19 inhib	CYP2C9 inhibi	CYP2D6 inhibi	CYP3A4 inhibi	Log Kp (skin per	Ghose	Egan	Muegge	Bioavailability S

				tor	**itor**	**tor**	**tor**	**tor**	**mentation, cm/s)**				**core**
TA1	High	Yes	No	Yes	No	Yes	No	Yes	-1.09	No	No	No	0.85
TA2	High	No	No	Yes	No	Yes	No	Yes	-0.75	No	No	No	0.85
TA3	High	Yes	No	Yes	No	Yes	No	Yes	-1.09	No	No	No	0.85
TA4	High	No	No	Yes	No	Yes	No	Yes	-1.03	No	No	No	0.85
TA5	High	Yes	No	Yes	No	Yes	No	Yes	-2.32	No	No	No	0.85
TA6	High	Yes	No	Yes	No	Yes	No	Yes	-1.38	No	No	No	0.85
TA7	High	No	No	Yes	No	Yes	No	Yes	-0.95	No	No	No	0.85
TA8	High	Yes	No	Yes	No	Yes	No	Yes	-1.26	No	No	No	0.85
TA9	High	Yes	No	Yes	No	Yes	No	Yes	-1.33	No	No	No	0.85
TA10	High	No	No	Yes	No	Yes	No	Yes	-0.9	No	No	No	0.85
TA11	High	Yes	No	Yes	No	Yes	No	Yes	-1.61	No	No	No	0.85
TA12	High	No	No	Yes	No	Yes	No	Yes	-1.35	No	No	No	0.85
TA13	High	No	No	Yes	No	Yes	No	Yes	-1.64	No	No	No	0.85
TA14	High	Yes	No	Yes	No	Yes	No	Yes	-1.61	No	No	No	0.85
TA15	High	No	No	Yes	No	Yes	No	Yes	-0.95	No	No	No	0.85
TA16	High	No	No	Yes	No	Yes	No	Yes	-2.11	No	No	No	0.85
TA17	High	No	No	Yes	No	Yes	Yes	Yes	-2.33	No	No	No	0.55
TA18	High	No	No	Yes	No	Yes	No	Yes	-2.03	No	No	No	0.55
TA19	High	No	No	Yes	No	Yes	No	Yes	-1.6	No	No	No	0.55
TA20	High	No	No	Yes	No	Yes	No	Yes	-2.05	No	No	No	0.85
TA21	High	No	No	Yes	No	Yes	No	Yes	-0.7	No	No	No	0.85
TA	Hi	No	No	Yes	No	Yes	No	Yes	-1.	No	No	No	0.

22	gh								06				85
TA23	High	No	No	Yes	No	Yes	No	Yes	-0.86	No	No	No	0.85
TA24	High	Yes	No	Yes	No	Yes	No	Yes	-1.05	No	No	No	0.85
TA25	High	Yes	No	Yes	No	Yes	No	Yes	-2.05	No	No	No	0.85
Trimethoprim	High	No	No	Yes	No	Yes	No	Yes	-3.58	No	No	No	0.55

GI abs.: Gastrointestinal absorption; BBB per.: Blood brain barrier permeate; P-gp sub.: P-glycoprotein substrate

***In-Silico* Toxicity analysis**

The in-silico toxicity profile of all synthesized thiazole derivatives (TA1-TA25) is shown in Table 4, which was predicted using the Geintox-II software (Geinforce Technology Pvt. Ltd., Pune). The majority of compounds (TA2, TA3, TA5, TA6, TA7, TA8, TA9, TA10, TA12, TA15, TA16, TA17, TA18, TA19, TA20, TA21, TA23, TA24) were classified under Toxicity Class 4 (harmful if swallowed), with LD50 values ranging from 300.0 to 533.5 mg/kg, while TA1, TA4, TA11, TA13, TA14, TA22, and TA25 fell under Class 3. All compounds were inactive with regard to carcinogen, muta gen and cytotoxicity prediction. For these derivatives, hepatotoxicity was considered as active in TA4, TA7, TA9, TA10 and TA22 and should be interpreted with caution. However, $P(\psi \gg)>K_{n}$, hepatotoxicity predictions were inactive for all other remaining compounds in this series with comparable hepatotoxicity predictions as that of Trimethoprim (LD50 = 1054.6 mg/kg Class 4) which confirmed the overall good hepatotoxicity safety predictions of this series as summarized in Table 4.

Table 4: Predicted toxicity of novel thiazole derivatives

Comp.	LD50	Toxici	Hepatotoxici	Carcinogenicity	Immunotoxicit	Mutagenicity	Cytotoxicit
Codes	(mg/kg)	ty Class	ty (Probability)	(Probability)	y (Probability)	(Probability)	y (Probability)
TA1	267.4	3	I (0.22)	I (0.25)	I (0.30)	I (0.12)	I (0.12)
TA2	423.8	4	I (0.24)	I (0.25)	I (0.10)	I (0.12)	I (0.12)
TA3	423.8	4	I (0.32)	I (0.25)	I (0.30)	I (0.12)	I (0.12)
TA4	267.4	3	A (0.60)	I (0.25)	I (0.30)	I (0.12)	I (0.12)
TA5	377.7	4	I (0.24)	I (0.25)	I (0.10)	I (0.12)	I (0.12)
TA6	336.6	4	I (0.20)	I (0.25)	I (0.30)	I (0.12)	I (0.12)
TA7	423.8	4	A (0.60)	I (0.25)	I (0.30)	I (0.12)	I (0.12)
TA8	336.6	4	I (0.22)	I (0.25)	I (0.30)	I (0.12)	I (0.12)
TA9	336.6	4	A (0.58)	I (0.25)	I (0.30)	I (0.12)	I (0.12)
TA10	423.8	4	A (0.52)	I (0.25)	I (0.10)	I (0.12)	I (0.12)
TA11	300.0	3	I (0.20)	I (0.25)	I (0.10)	I (0.12)	I (0.12)
TA12	423.8	4	I (0.21)	I (0.25)	I (0.10)	I (0.12)	I (0.12)
TA13	300.0	3	I (0.19)	I (0.25)	I (0.10)	I (0.12)	I (0.12)

TA 14	300.0	3	I (0.20)	I (0.25)	I (0.10)	I (0.12)	I (0.12)
TA 15	5335	4	I (0.32)	I (0.25)	I (0.10)	I (0.12)	I (0.12)
TA 16	3777	4	I (0.25)	I (0.25)	I (0.10)	I (0.12)	I (0.12)
TA 17	3777	4	I (0.25)	I (0.25)	I (0.10)	I (0.12)	I (0.12)
TA 18	3777	4	I (0.26)	I (0.25)	I (0.10)	I (0.12)	I (0.12)
TA 19	423.8	4	I (0.30)	I (0.25)	I (0.30)	I (0.12)	I (0.12)
TA 20	3777	4	I (0.26)	I (0.25)	I (0.10)	I (0.12)	I (0.12)
TA 21	423.8	4	I (0.32)	I (0.25)	I (0.30)	I (0.12)	I (0.12)
TA 22	267.4	3	A (0.60)	I (0.25)	I (0.30)	I (0.12)	I (0.12)
TA 23	336.6	4	I (0.32)	I (0.25)	I (0.30)	I (0.12)	I (0.12)
TA 24	423.8	4	I (0.22)	I (0.25)	I (0.10)	I (0.12)	I (0.12)
TA 25	300.0	3	I (0.17)	I (0.25)	I (0.10)	I (0.12)	I (0.12)
Trimethoprim	1054.6	4	I (0.12)	I (0.10)	I (0.10)	I (0.12)	I (0.12)

A = Active; I = Inactive

Validation of docking protocol

Prior to molecular docking, the docking protocol was validated by redocking the co-crystallized ligand into the active site of DHFR (PDB ID: 1AJ2). The superimposition of the co-crystallized (green) and redocked pose (purple) demonstrated excellent spatial agreement, yielding an RMSD value of 1.42 Å (Figure 2), confirming the reliability and accuracy of the employed docking protocol.

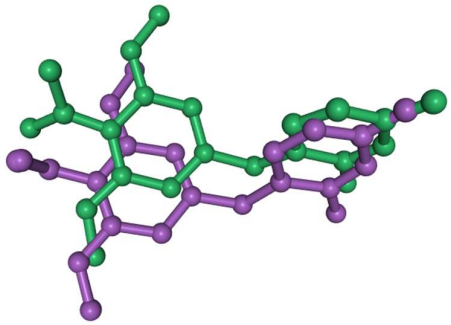

Figure 2: Superimposition of co-crystallized ligand (green) and redocked pose (purple) within the active site of DHFR (PDB ID: 1AJ2) demonstrating docking protocol validation; RMSD = 1.42 Å.

8.5. Results of Molecular Docking

Table 5 shows all the synthesized thiazole derivatives (TA1 – TA25) results after docking with DHFR (PDB ID: 1AJ2) as well as a reference drug Trimethoprim. The scoring for all compounds showed good scores which are greater than Trimethoprim with a score of -7.056 kcal/mol which suggests better scores towards the active site of DHFR. The docking scores placed the TA22, TA13, TA19, TA11 and TA7 as the top five scores in the series with Scores ranging from −8.380 kcal/mol (TA17) to −9.361 kcal/mol (TA22). The active site residues involved in the majority of the compounds were the same and included THR46, ILE14, LYS45, LEU20, PHE92, ALA7, VAL6, ASN18 and THR121 with a conserved binding mode in the catalytic pocket of DHFR. As shown in Figures 3A and 3B, the hydrogen bond between TA13 (−9.356 kcal/mol) and THR46, ALA7 and VAL6 as well as electrostatic and hydrophobic interactions were formed. TA19 (−9.293 kcal/mol) showed a variety of interactions including hydrogen bond, electrostatic, hydrophobic, and also a halogen bond and Pi-Sulfur bond (Figures 4A and 4B). The highest-scoring compound, TA22 (−9.361 kcal/mol), showed multiple hydrogen bonds and halogen bond contacts with ILE14, THR46, ASN18, THR121 and ASP120, as shown in Figures 5A and 5B. Trimethoprim made hydrogen bond, electrostatic, and hydrophobic contacts with ALA7, ASP27, PHE92 and SER49, and was used as a model to compare binding assessment.

Table 5: Molecular docking interaction analysis of novel thiazole derivatives (TA1–TA25) against DHFR (PDB ID: 1AJ2) with Trimethoprim as reference standard.

Compound	Active Amino	Bond Lengths (Å)	Bond Categories	Docking Score

	Residues			**(kcal/mol)**
TA1	ILE14, THR46, LYS45, LEU20, VAL6, PHE92, ALA7, ASP27, ASN18, THR121, PHE98, GLY94	2.33, 3.12, 5.12, 3.74, 4.35, 4.86, 5.07, 5.10, 5.34, 3.36, 3.44, 3.49, 3.69, 3.82	Hydrogen Bond, Electrostatic, Hydrophobic, Halogen Bond, Van der Waals	−9.211
TA2	GLN95, THR46, THR96, ASP27, ILE14, LYS45, LEU20, PHE92, VAL31, LEU28, THR121, GLY94, LEU5, VAL6	3.06, 3.30, 2.98, 2.98, 2.99, 4.03, 4.34, 4.59, 4.95, 3.55, 3.85, 3.47, 3.61, 3.71, 3.79	Hydrogen Bond, Hydrophobic, Van der Waals	−8.941
TA3	ILE14, THR46, LYS45, LEU20, VAL6, PHE98, ASN18, ALA7, THR121, PHE92, ASP120	2.43, 3.14, 5.09, 3.87, 4.12, 5.46, 3.12, 3.28, 3.44, 3.50, 3.54, 3.69, 3.82	Hydrogen Bond, Electrostatic, Hydrophobic, Van der Waals	−8.765
TA4	THR46, ASN18, THR121, LYS45, LEU20, ILE14, PHE92, ASP27, VAL31, PHE98, ALA7, LEU28, GLN95, GLY94, VAL6	2.62, 2.75, 2.95, 5.20, 3.55, 4.67, 5.04, 5.27, 3.00, 3.30, 3.34, 3.45, 3.53, 3.55, 3.56, 3.87	Hydrogen Bond, Electrostatic, Hydrophobic, Van der Waals	−8.940
TA5	ILE14, THR46, LEU5, LYS45, LEU20, VAL31, ALA7, LEU28,	2.88, 3.04, 2.70, 4.01, 4.12, 4.94, 5.12, 5.41, 3.85, 3.28, 3.44, 4.81, 3.09, 3.33, 3.33, 3.37,	Hydrogen Bond, Hydrophobic, Halogen Bond, Pi-Sulfur, Van der Waals	−8.857

	GLN 95, GLN 19, PHE92, ASN18, ASP120, THR121, GLY94, GLY15, VAL6, ASP27	3.57, 3.69, 3.72		
TA6	ALA 7, THR121, THR46, ASN18, LYS45, LEU20, ILE14, PHE92, LEU28, VAL31, LEU5, VAL6, ASP27, GLY94	3.12, 3.27, 3.33, 2.60, 5.63, 3.70, 3.93, 5.00, 5.24, 5.48, 5.50, 3.53, 3.16, 3.19, 3.34, 3.60	Hydrogen Bond, Electrostatic, Hydrophobic, Halogen Bond, Van der Waals	−9.117
TA7	THR46, ASP27, LYS45, PHE92, LEU20, ILE14,	2.89, 2.57, 5.75, 3.58, 4.15, 4.37, 5.10, 5.27, 3.88, 3.94, 3.47, 3.63	Hydrogen Bond, Electrostatic, Hydrophobic, Van der Waals	−9.228
	PHE98, ALA7, VAL6, THR121, ASN18			
TA8	THR121, ASN18, LEU5, LYS45, LEU20, PHE92, ILE14, ALA7, VAL6, VAL31, ASP27, THR46, GLY94, GLN95	3.22, 2.55, 2.85, 5.61, 3.70, 4.45, 4.66, 4.94, 5.11, 5.22, 3.72, 3.30, 3.12, 3.45, 3.64, 3.70	Hydrogen Bond, Electrostatic, Hydrophobic, Halogen Bond, Van der Waals	−9.017
TA9	ILE14, THR46, ASP27, ASN18, LYS45, LEU20, PHE92, VAL31, ALA7, LEU5, VAL6,	2.40, 2.83, 2.53, 3.00, 4.67, 3.43, 3.49, 4.74, 5.29, 3.66, 3.68, 2.88, 3.21, 3.22, 3.48	Hydrogen Bond, Electrostatic, Hydrophobic, Van der Waals	−8.700

	GLY94, THR121			
TA10	GLN95, THR46, THR96, LYS45, LEU20, ILE50, PHE92, ILE14, LEU28, LEU54, VAL31, THR121, ASP27, GLY94	3.06, 3.07, 2.99, 4.05, 4.26, 4.80, 4.84, 5.04, 3.56, 3.62, 3.79, 3.48, 3.58, 3.59	Hydrogen Bond, Hydrophobic, Van der Waals	−8.731
TA11	LEU28, LYS32, LEU54, LEU20, ILE14, VAL31, PHE92, ILE50	2.76, 5.76, 3.74, 3.86, 4.19, 4.37, 4.47, 4.83, 4.95, 5.11	Hydrogen Bond, Electrostatic, Hydrophobic	−9.283
TA12	LYS45, ALA7, VAL31, LEU20, LEU5, ILE14, VAL6	4.84, 3.61, 4.22, 4.35, 4.63, 4.87, 5.00, 5.12, 3.29, 3.45, 3.45, 3.58,	Electrostatic, Hydrophobic, Van der Waals	−9.247
	, THR121, ASP27, PHE92, GLY94, ASN18, THR46	3.60, 3.74		
TA13	THR46, ALA7, VAL6, LYS45, PHE92, LEU20, VAL31, ILE14, LEU5, THR121, ASN18, GLY94	2.82, 3.11, 2.91, 5.05, 3.97, 4.05, 4.09, 4.55, 4.65, 4.84, 5.41, 3.35, 3.48, 3.72	Hydrogen Bond, Electrostatic, Hydrophobic, Van der Waals	−9.356
TA14	ILE14, THR121, THR46, THR96, LEU5, PHE92, LYS45, LEU20, VAL31, ALA7, LEU28, ASN1	3.06, 3.12, 3.16, 2.09, 2.79, 4.44, 4.05, 4.28, 4.73, 5.14, 5.30, 3.76, 4.85, 3.47, 3.62, 3.67, 3.77	Hydrogen Bond, Hydrophobic, Pi-Sulfur, Van der Waals	−9.173

	8, ASP27, GLN95, VAL6			
TA15	THR46, PHE92, LEU54, LEU28, LEU20, ILE50, LYS32, VAL31, ILE14, GLY94, THR121	3.02, 2.94, 3.77, 3.80, 4.45, 4.65, 4.78, 4.94, 5.02, 5.43, 3.72, 3.73	Hydrogen Bond, Hydrophobic, Van der Waals	−9.229
TA16	THR46, ALA7, ASP120, LYS45, LEU20, ILE14, VAL6, LEU28, PHE92, PHE98, THR121, LEU5, ASN18, ASP27, GLY94	2.90, 3.08, 2.88, 5.01, 4.08, 4.19, 4.74, 5.50, 3.67, 4.66, 3.24, 3.35, 3.47, 3.52, 3.54, 3.79	Hydrogen Bond, Electrostatic, Hydrophobic, Pi-Sulfur, Van der Waals	−8.957
TA17	THR46, ASN18, ARG57, LEU28, LEU54, PHE92, LEU20, ILE50, VAL31, LYS32, LYS45, ILE14, GLY94, THR121, GLY93, PHE98	5.95, 3.44, 3.62, 3.70, 4.16, 4.75, 4.87, 3.37, 3.74, 3.01, 3.33, 3.47, 3.84, 3.92	Electrostatic, Hydrophobic, Van der Waals	−8.380
TA18	THR46, ILE14, ASP120, LEU5, LYS45, LEU20, VAL31, ALA7, LEU28, PHE92, THR121, GLN95, VAL6, ASP27, ASN18,	3.15, 3.38, 2.86, 2.87, 3.88, 4.32, 5.01, 5.13, 5.45, 3.97, 4.80, 3.39, 3.65, 3.71, 3.79, 3.81, 3.90	Hydrogen Bond, Hydrophobic, Pi-Sulfur, Van der Waals	−8.880

	GLY94			
TA19	THR46, LYS45, LEU20, PHE98, ILE14, ILE50, VAL6, LEU28, ALA7, PHE92, THR121, ASN18	2.85, 5.76, 3.63, 4.51, 5.01, 5.17, 3.44, 3.83, 3.92, 3.05, 4.91, 3.40, 3.64	Hydrogen Bond, Electrostatic, Hydrophobic, Halogen Bond, Pi-Sulfur, Van der Waals	−9.293
TA20	THR46, THR96, LEU5, LYS45, LEU20, ILE14, VAL31, ALA7, PHE92, GLN95, ASN18, THR121, GLY94, VAL6	2.26, 3.10, 3.49, 2.74, 5.92, 3.63, 4.56, 4.99, 5.04, 5.10, 3.70, 4.59, 3.08, 3.25, 3.32, 3.58, 3.69	Hydrogen Bond, Electrostatic, Hydrophobic, Pi-Sulfur, Van der Waals	−8.916
TA21	THR46, ILE14, LEU28, LEU5	2.61, 2.97, 3.62, 4.01, 4.25, 4.65, 4.97,	Hydrogen Bond, Hydrophobic, Van der Waals	−9.220
	4, LEU20, PHE92, VAL31, ILE50, LYS32, PHE98, VAL6, ALA7	5.24, 5.27, 5.33, 3.05, 3.45		
TA22	ILE14, THR46, ASN18, THR121, ASP120, LYS45, LEU20, PHE92, ALA7, VAL31, ASP27, LEU5, GLY94, VAL6	2.53, 2.96, 2.28, 2.69, 2.88, 2.97, 5.26, 3.60, 3.88, 5.11, 5.14, 5.15, 3.74, 3.19, 3.06, 3.45, 3.66	Hydrogen Bond, Electrostatic, Hydrophobic, Halogen Bond, Van der Waals	−9.361
TA23	PHE92, THR46, LEU28, ARG57, LEU54, LEU20, LYS32, VAL31,	2.69, 2.73, 2.94, 5.94, 3.76, 3.85, 4.13, 4.44, 4.78, 4.85, 3.82, 3.31, 3.28, 3.40, 3.49	Hydrogen Bond, Electrostatic, Hydrophobic, Halogen Bond, Van der Waals	−8.891

	ILE50, ALA 7, VAL6, ILE14, PHE98			
TA24	GLN 95, THR46, LEU5, ILE14, LYS45, PHE92, LEU20, ALA 7, VAL6, THR96, THR121, VAL31, LEU28, GLY94	3.07, 3.36, 2.69, 2.93, 4.00, 4.47, 4.47, 4.91, 3.92, 3.41, 3.48, 3.49, 3.50, 3.51, 3.65	Hydrogen Bond, Hydrophobic, Van der Waals	−8.814
TA25	LYS45, PHE92, LEU20, ILE14, VAL6, ALA 7, VAL31, LEU5, THR121, ASN18, THR46, ASP27, GLY94, PHE98	4.84, 3.84, 4.75, 4.76, 4.88, 5.42, 3.47, 3.72, 2.94, 3.34, 3.57, 3.62, 3.72, 3.75, 3.86	Electrostatic, Hydrophobic, Van der Waals	−8.741
Trimethoprim	ALA 7, THR121, SER49, ASP27, PHE92, PHE98, LEU20, ILE14, VAL6, GLY15, ASN18, GLN 95, GLY94, GLN 19	1.91, 3.33, 3.36, 3.45, 2.95, 5.90, 5.95, 5.28, 4.23, 4.75, 4.89, 5.04, 5.39, 3.47, 3.50, 3.53, 3.67, 3.68	Hydrogen Bond, Electrostatic, Hydrophobic, Van der Waals	−7.056

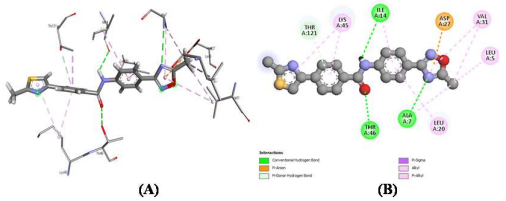

Figure 3: Molecular docking interaction plots of TA13 with DHFR (PDB ID: 1AJ2); (A) 3D interaction plot and (B) 2D interaction plot.

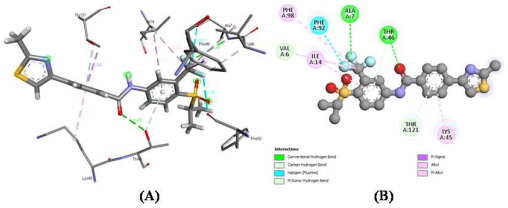

Figure 4: Molecular docking interaction plots of TA19 with DHFR (PDB ID: 1AJ2); (A) 3D interaction plot and (B) 2D interaction plot.

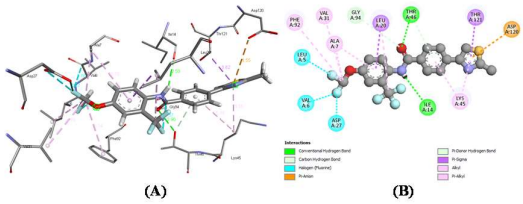

Figure 5: Molecular docking interaction plots of TA22 with DHFR (PDB ID: 1AJ2); (A) 3D interaction plot and (B) 2D interaction plot.

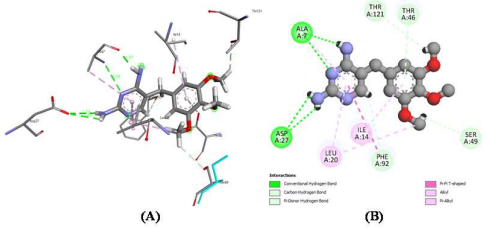

Figure 6: Molecular docking interaction plots of Trimethoprim (co-crystallized reference standard) with DHFR (PDB ID: 1AJ2); (A) 3D interaction plot and (B) 2D interaction plot.

Discussion

The analysis for drug-likeness of synthesized thiazole derivatives (TA1-TA25) by using Lipinski's rule of five and Veber's rule showed that all thiazole derivatives had molecular weights of < 500 g/mol, MLogP within acceptable range, TPSA and rotatable bond count (Table 2). The uniform presence of one such violation in this series is supportive of the fortuitous observation reported with the halogenated benzamide scaffolds that one violation is acceptable without impairing oral bioavailability. The use of the hybrid thiazole-benzamide structure in the present series has been correlated with desirable physicochemical space in the past and the present observations confirm this. Interestingly, there was a lower rotatable bond count of Trimethoprim (10) compared with that of the reference standard (14) and the group exhibited comparatively higher TPSA (105.51 Å²) than the reference standard [34, 35].

The in-silico ADME analysis (Table 3) showed uniformly strong gastrointestinal (GI) absorption as well as lack of P-glycoprotein (PGP) substrate recognition for all 25 compounds, which were considered good characteristics for oral delivery of antibacterial candidates. Previously documented for structurally related thiazole-containing scaffolds, the series showed constant inhibition of the CYP1A2, CYP2C9 and CYP3A4 isoforms, suggesting an effect of the electron-withdrawing substituents in the binding of metabolic enzymes of the series. The selective CYP2D6 inhibitory effect noted only for TA17 could be due to the presence of the dimethylaminosulfonyl substitution pattern of this compound and should be taken into account during lead optimization [36]. The bioavailability score was found to be 0.85 for most of the compounds which is found to be good when compared with Trimethoprim (0.55) also the majority of compounds in the vast series were found to be pharmaceutical. Ten compounds are predicted candidates for BBB penetration by them, which is consistent with the lipophilic nature of the trifluoromethyl and fluoroalkoxy groups which have been associated with CNS penetration in related fluorinated aromatic series [37, 38].

The ADMET profile predicted by Geintox-II (Table4) showed that all the derivatives are carcinogenic, mutagenic and cytotoxic inactive suggesting their safety profiles as reported in the published literature for the thiazole scaffold based antibacterial candidates [39]. The hepatotoxicity prediction functions were active for TA4, TA7, TA9, TA10, and TA22, probably due to the presence of highly lipophilic trifluoromethoxy and cyclopropylmethoxy substituents which have been previously associated with higher hepatotoxicity risk for a class of halogenated aromatic compounds. All the other twenty compounds displayed inactive hepatotoxicity indicating their relatively safety when compared to the reference drug Trimethoprim (LD50 = 1054.6 mg/kg Class 4) [40–42].

The molecular docking studies of all synthesized compounds against DHFR (PDB ID: 1AJ2) showed that all the compounds were able to bind the receptor better than Trimethoprim (−7.056 kcal/mol) with binding affinity ranging from −8.380 to −9.361 kcal/mol (Table 5). TA22 (−9.361 kcal/mol), TA13 (−9.356 kcal/mol), and TA19 (−9.293 kcal/mol) were found as the most-affine compounds with various interaction types, such as hydrogen bonding and halogen bonding, as well as electrostatic contact with THR46, ILE14, LYS45, and PHE92 residues used in the binding of DHFR inhibitors containing electronwithdrawing aryl groups (Figures 3–6) [43, 44]. Both the docking protocol reliability and RMSD value by redocking validation (1.42 Å) disclosed in Figure 2 confirmed the reliability of the docking protocol. An important limitation of the present study is that all the findings were based solely on computational predictions and so experimental validation using in vitro antibacterial assays, enzyme inhibition testing, and cytotoxicity testing of the synthesized compounds is needed to validate the in-silico findings [45].

Conclusion

To conclude, a series of 25 novel thiazole-benzamide hybrid derivatives (TA1- TA25) was designed, synthesized and their activities have been comprehensively evaluated through in-silico studies of DHFR as an antibacterial target. The drug-likeness parameters were found to be favorable for all the compounds within the limit of Lipinski's rule and Veber's rule and their GIT absorption was high, along with acceptable predicted toxicity profile, thus the compounds can be considered to be pharmacologically suitable for use as novel oral antibacterial agents. Molecular docking study showed that, TA22, TA13 and TA19 showed a high

binding affinity to DHFR (PDB ID: 1AJ2) as compared to reference standard Trimethoprim, in which these candidates participate with hydrogen bond, halogen bond, electrostatic interaction with the key catalytic residues of the enzyme which implies their ability to inhibit bacterial folate synthesis and overcome the present bacterial resistance mechanism. The results serve as a good starting point for the future development of the thiazole-benzamide scaffold; future in vitro antibacterial screening and enzyme inhibition studies and in vivo pharmacological evaluation will be warranted on this computational observation and turned into therapy-worthy antibacterial candidates.

Abbreviations

DHFR: Dihydrofolate reductase; FT-IR: Fourier-transform infrared spectroscopy; NMR: Nuclear magnetic resonance; ESI-MS: Electrospray ionization mass spectrometry; ADME: Absorption, distribution, metabolism, and excretion; TPSA: Total polar surface area; MLogP: Moriguchi octanol-water partition coefficient; HBA: Hydrogen bond acceptors; HBD: Hydrogen bond donors; GI: Gastrointestinal; BBB: Blood-brain barrier; P-gp: P-glycoprotein; CYP: Cytochrome P450; Log Kp: Logarithm of skin permeation coefficient; LD50: Lethal dose fifty; PDB: Protein data bank; RMSD: Root mean square deviation; DCM: Dichloromethane; $CDCl_3$: Deuterated chloroform; SAR: Structure-activity relationship; SMILES: Simplified molecular input line entry system; QSAR: Quantitative structure-activity relationship; MHz: Megahertz; ppm: Parts per million; kcal/mol: Kilocalories per mole; Å: Angstrom; g/mol: Grams per mole; OPC: One person company; DNA: Deoxyribonucleic acid; WHO: World Health Organization; MDR: Multidrug resistant; IUPAC: International union of pure and applied chemistry; KBr: Potassium bromide; THF: Tetrahydrofuran; $SOCl_2$: Thionyl chloride; Et_3N: Triethylamine.

References

1. Murray, C. J. L., Ikuta, K. S., Sharara, F., Swetschinski, L., Aguilar, G. R., Gray, A., … Naghavi, M. (2022). Global burden of bacterial antimicrobial resistance in 2019: a systematic analysis. *The Lancet*, *399*(10325), 629–655. https://doi.org/10.1016/S0140-6736(21)02724-0
2. Liu, H. Y., Prentice, E. L., & Webber, M. A. (2024). Mechanisms of antimicrobial resistance in biofilms. *npj Antimicrobials and Resistance*, *2*(1), 27. https://doi.org/10.1038/s44259-024-00046-3
3. Darby, E. M., Trampari, E., Siasat, P., Gaya, M. S., Alav, I., Webber, M. A., & Blair, J. M. A. (2023). Molecular mechanisms of antibiotic resistance revisited. *Nature Reviews Microbiology*, *21*(5), 280–295. https://doi.org/10.1038/s41579-022-00820-y
4. Liu, H. Y., Prentice, E. L., & Webber, M. A. (2024). Mechanisms of antimicrobial resistance in biofilms. *npj Antimicrobials and Resistance*, *2*(1), 27. https://doi.org/10.1038/s44259-024-00046-3
5. Dawood, K. M., Raslan, M. A., Abbas, A. A., Mohamed, B. E., Abdellattif, M. H., Nafie, M. S., & Hassan, M. K. (2021). Novel Bis-Thiazole Derivatives: Synthesis and Potential Cytotoxic Activity Through Apoptosis With Molecular Docking Approaches. *Frontiers in Chemistry*, *9*. https://doi.org/10.3389/fchem.2021.694870
6. Liu, H., Xu, T., Xue, Z., Huang, M., Wang, T., Zhang, M., … Guo, Y. (2024). Current Development of Thiazole-Containing Compounds as Potential Antibacterials against Methicillin-Resistant Staphylococcus aureus. *ACS infectious diseases*, *10*(2), 350–370. https://doi.org/10.1021/acsinfecdis.3c00647
7. Mohammad, H., Cushman, M., & Seleem, M. N. (2015). Antibacterial Evaluation of Synthetic Thiazole Compounds In Vitro and In Vivo in a Methicillin-Resistant Staphylococcus aureus (MRSA) Skin Infection Mouse Model. *PLOS ONE*, *10*(11), e0142321. https://doi.org/10.1371/journal.pone.0142321
8. Niu, Z.-X., Wang, Y.-T., Zhang, S.-N., Li, Y., Chen, X.-B., Wang, S.-Q., & Liu, H.-M. (2023). Application and synthesis of thiazole ring in clinically approved drugs. *European Journal of Medicinal Chemistry*, *250*, 115172. https://doi.org/10.1016/j.ejmech.2023.115172
9. Rahane, D. R. D., Shirke, M. S. B., Kadam, P. V. N., Musale, M. Y. J., Tandale, M. A. S., Nimase, M. P. A., & Sable, P. J. V. (2025). Synthesis and characterization of Thieno[3,2-d]pyrimidine Derivatives for Antimicrobials activity. *International Journal of Environmental Sciences*, 886–900. https://doi.org/10.64252/7y5s5w09
10. Guo, J., Xie, Z., Ruan, W., Tang, Q., Qiao, D., & Zhu, W. (2023). Thiazole-based analogues as potential antibacterial agents against methicillin-resistant Staphylococcus aureus (MRSA) and their SAR elucidation. *European Journal of Medicinal Chemistry*, *259*, 115689. https://doi.org/10.1016/j.ejmech.2023.115689
11. Cascioferro, S., Parrino, B., Carbone, D., Schillaci, D., Giovannetti, E., Cirrincione, G., & Diana, P. (2020). Thiazoles, Their Benzofused Systems, and Thiazolidinone Derivatives: Versatile and Promising Tools to Combat Antibiotic Resistance. *Journal of Medicinal Chemistry*, *63*(15), 7923–7956.

https://doi.org/10.1021/acs.jmedchem.9b01245

12. Arshad, M. F., Alam, A., Alshammari, A. A., Alhazza, M. B., Alzimam, I. M., Alam, M. A., … Jomah, S. (2022). Thiazole: A Versatile Standalone Moiety Contributing to the Development of Various Drugs and Biologically Active Agents. *Molecules*, *27*(13), 3994. https://doi.org/10.3390/molecules27133994
13. Lemilemu, F., Bitew, M., Demissie, T. B., Eswaramoorthy, R., & Endale, M. (2021). Synthesis, antibacterial and antioxidant activities of Thiazole-based Schiff base derivatives: a combined experimental and computational study. *BMC Chemistry*, *15*(1), 67. https://doi.org/10.1186/s13065-021-00791-w
14. Technology, G. (n.d.). Geinforce Technology - Advanced Drug Discovery Tools. Retrieved July 4, 2026, from http://geinforce.com/documentation/?utm_source=chatgpt.com
15. Martin, Y. C. (2005). A bioavailability score. *Journal of Medicinal Chemistry*, *48*(9), 3164–3170. https://doi.org/10.1021/jm0492002
16. Ghose, A. K., Viswanadhan, V. N., & Wendoloski, J. J. (1999). A knowledge-based approach in designing combinatorial or medicinal chemistry libraries for drug discovery. 1. A qualitative and quantitative characterization of known drug databases. *Journal of Combinatorial Chemistry*, *1*(1), 55–68. https://doi.org/10.1021/cc9800071
17. Geinforce Technology - AI-Driven Drug Discovery. (n.d.). Retrieved July 4, 2026, from https://geinforce.com/
18. Dalby, A., Nourse, J. G., Hounshell, W. D., Gushurst, A. K. I., Grier, D. L., Leland, B. A., & Laufer, J. (1992). Description of several chemical structure file formats used by computer programs developed at Molecular Design Limited. *Journal of Chemical Information and Computer Sciences*, *32*(3), 244–255. https://doi.org/10.1021/ci00007a012
19. ChemDraw | Revvity Signals Software. (n.d.). Retrieved July 4, 2026, from https://revvitysignals.com/products/research/chemdraw?utm_source=chatgpt.com
20. Dawood, D. H., Sayed, M. M., Tohamy, S. T. K., & Nossier, E. S. (2023). New Thiophenyl-pyrazolyl-thiazole Hybrids as DHFR Inhibitors: Design, Synthesis, Antimicrobial Evaluation, Molecular Modeling, and Biodistribution Studies. *ACS omega*, *8*(42), 39250–39268. https://doi.org/10.1021/acsomega.3c04736
21. Wróbel, A., Arciszewska, K., Maliszewski, D., & Drozdowska, D. (2020). Trimethoprim and other nonclassical antifolates an excellent template for searching modifications of dihydrofolate reductase enzyme inhibitors. *The Journal of Antibiotics*, *73*(1), 5–27. https://doi.org/10.1038/s41429-019-0240-6
22. Visualization. (2023, September 14). *Dassault Systèmes*. Retrieved July 4, 2026, from https://www.3ds.com/products/biovia/discovery-studio/visualization
23. GeinDock Suite - Web-Based Molecular Docking Platform. (n.d.). Retrieved July 4, 2026, from https://geindock.geinforce.com/?__cf_chl_f_tk=f.wN9d1XZX5yNYyvCJ2TpN7f_jZaj2BNWlddAFeH1uM-1783156637-1.0.1.1-1swsjray3vPS4JAXfY6aEVjjgdtBIWAx5jedyxvKFGE
24. Visualization. (2023, September 14). *Dassault Systèmes*. Retrieved July 4, 2026, from https://www.3ds.com/products/biovia/discovery-studio/visualization
25. Abumelha, H. M., Sefrji, F. O., Alrefaei, A. F., Mojally, M., Alotaibi, F. A., Alomari, K. B., … El-Metwaly, N. M. (2025). Exploring Thiazole-Based Heterocycles: Synthesis, Bioactivity, and Molecular Docking for Antimicrobial Applications. *Chemical Biology & Drug Design*, *105*(5), e70124. https://doi.org/10.1111/cbdd.70124
26. Althagafi, I., El-Metwaly, N., & Farghaly, T. A. (2019). New Series of Thiazole Derivatives: Synthesis, Structural Elucidation, Antimicrobial Activity, Molecular Modeling and MOE Docking. *Molecules*, *24*(9), 1741. https://doi.org/10.3390/molecules24091741
27. Kartsev, V., Geronikaki, A., Zubenko, A., Petrou, A., Ivanov, M., Glamočlija, J., … Klimenko, A. (2022). Synthesis and Antimicrobial Activity of New Heteroaryl(aryl) Thiazole Derivatives Molecular Docking Studies. *Antibiotics*, *11*(10), 1337. https://doi.org/10.3390/antibiotics11101337
28. Matta, R., Pochampally, J., Dhoddi, B. N., Bhookya, S., Bitla, S., & Akkiraju, A. G. (2023). Synthesis, antimicrobial and antioxidant activity of triazole, pyrazole containing thiazole derivatives and molecular docking studies on COVID-19. *BMC Chemistry*, *17*(1), 61. https://doi.org/10.1186/s13065-023-00965-8
29. El-Naggar, A. M., Zidan, A., Elkaeed, E. B., Taghour, M. S., & Badawi, W. A. (2022). Design, synthesis and docking studies of new hydrazinyl-thiazole derivatives as anticancer and antimicrobial agents. *Journal of Saudi*

Chemical Society, *26*(4), 101488. https://doi.org/10.1016/j.jscs.2022.101488

30. Mehdhar, F. S., Abdel-Latif, E., Abdel-Galil, E., & Abdel-Ghani, G. E. (2026). Design, Synthesis, and Biological Evaluation of Some New Thiazole-Based Compounds as Antioxidant and Antimicrobial Agents. *Journal of Heterocyclic Chemistry*, *63*(4), 567–578. https://doi.org/10.1002/jhet.70155
31. Marufa, S. S., Sneegdha, J. J., Hossain, Md. F., Ahmed, Md. S., Islam, Z., Debnath, J. R., … Haque, Md. A. (2026). Novel Carbazole-Thiazole-Schiff Base Hybrids: Design, Synthesis, Antimicrobial, Antioxidant, Molecular Docking and Dynamics Studies. *Chemistry Africa*, *9*(2), 82. https://doi.org/10.1007/s42250-026-01589-w
32. Emad Abd El-Ghani, G., Mahmoud El-Sayed, S., Fikry El-Sayed, A., & Gamal El-Bana, G. (2026). Design, Synthesis, Biological Evaluation and In-Silico Investigation, Molecular Docking, Molecular Dynamics Simulations, and ADMET Profiling of Novel Thiazole-Based Derivatives. *Polycyclic Aromatic Compounds*, *46*(3), 303–333. https://doi.org/10.1080/10406638.2025.2587067
33. Ahmed, A. T., & Hussein, A. J. (2026). Novel thiazole–imine hybrids: one pot and stepwise synthesis, characterization, antibacterial, antioxidant activities, and molecular docking studies. *Journal of Sulfur Chemistry*, *47*(1), 35–54. https://doi.org/10.1080/17415993.2025.2575780
34. Veber, D. F., Johnson, S. R., Cheng, H.-Y., Smith, B. R., Ward, K. W., & Kopple, K. D. (2002). Molecular properties that influence the oral bioavailability of drug candidates. *Journal of Medicinal Chemistry*, *45*(12), 2615–2623. https://doi.org/10.1021/jm020017n
35. Lipinski, C. A., Lombardo, F., Dominy, B. W., & Feeney, P. J. (2001). Experimental and computational approaches to estimate solubility and permeability in drug discovery and development settings. *Advanced drug delivery reviews*, *46*(1–3), 3–26. https://doi.org/10.1016/s0169-409x(00)00129-0
36. Daina, A., Michielin, O., & Zoete, V. (2017). SwissADME: a free web tool to evaluate pharmacokinetics, drug-likeness and medicinal chemistry friendliness of small molecules. *Scientific Reports*, *7*(1), 42717. https://doi.org/10.1038/srep42717
37. Siddheshwar, S. S., Jadhav, Mr. A. M., Mankar, S. D., Ghorpade, A. C., & Bhalerao, P. (2026). Development and optimization of avanafil cocrystals: in silico molecular docking approach for enhanced aqueous solubility and dissolution rate. *Journal of Molecular Structure*, *1351*, 144281. https://doi.org/10.1016/j.molstruc.2025.144281
38. Sun, S., & Adejare, A. (2006). Fluorinated molecules as drugs and imaging agents in the CNS. *Current Topics in Medicinal Chemistry*, *6*(14), 1457–1464. https://doi.org/10.2174/156802606777951046
39. Bank, R. P. D. (n.d.). RCSB PDB - 1AJ2: CRYSTAL STRUCTURE OF A BINARY COMPLEX OF E. COLI DIHYDROPTEROATE SYNTHASE. Retrieved July 4, 2026, from https://www.rcsb.org/structure/1AJ2
40. Bhandari, S. V., Nagras, O. G., Patil, S. M., Shimpi, Y., Chaudhari, S. Y., & Pawar, S. C. (2026). Exploring Ionic Liquid-Based Methods in the Synthesis of Benzimidazole-1,3,4-Oxadiazole Derivatives for EGFR Inhibition, designed using a Comprehensive Molecular Docking and Dynamics Study. *Journal of Molecular Structure*, *1351*, 143981. https://doi.org/10.1016/j.molstruc.2025.143981
41. Technology, G. (n.d.). Geinforce Technology - Advanced Drug Discovery Tools. Retrieved July 4, 2026, from http://geinforce.com/documentation/
42. Jaladanki, C. K., Khatun, S., Gohlke, H., & Bharatam, P. V. (2021). Reactive Metabolites from Thiazole-Containing Drugs: Quantum Chemical Insights into Biotransformation and Toxicity. *Chemical Research in Toxicology*, *34*(6), 1503–1517. https://doi.org/10.1021/acs.chemrestox.0c00450
43. Lamb, K. M., G-Dayanandan, N., Wright, D. L., & Anderson, A. C. (2013). Elucidating features that drive the design of selective antifolates using crystal structures of human dihydrofolate reductase. *Biochemistry*, *52*(41), 10.1021/bi400852h. https://doi.org/10.1021/bi400852h
44. Pantsar, T., & Poso, A. (2018). Binding Affinity via Docking: Fact and Fiction. *Molecules : A Journal of Synthetic Chemistry and Natural Product Chemistry*, *23*(8), 1899. https://doi.org/10.3390/molecules23081899
45. Yusuf, D., Davis, A. M., Kleywegt, G. J., & Schmitt, S. (2008). An Alternative Method for the Evaluation of Docking Performance: RSR vs RMSD. *Journal of Chemical Information and Modeling*, *48*(7), 1411–1422. https://doi.org/10.1021/ci800084x